Refereed Proceedings

The 12th International Conference on Fluidization - New Horizons in Fluidization Engineering

Engineering Conferences International *Year* 2007

Gas-Solid Structure in the Vicinity of a Sparger Nozzle in a Fluidized Bed

Pierre Sauriol* Heping Cui†

Jamal Chaouki‡

*École Polytechnique de Montréal, pierre.sauriol@polymtl.ca

†University of British Columbia

‡Ecole Polytechnique Montreal, jamal.chaouki@polymtl.ca

GAS-SOLID STRUCTURE IN THE VICINITY OF A SPARGER NOZZLE IN A FLUIDIZED BED

Pierre Sauriol[1], Heping Cui[2] and Jamal Chaouki[1]
1) Department of Chemical Engineering, École Polytechnique de Montréal,
C.P. 6079, succ. Centre-Ville, Montréal, Québec, H3C 3A7, Canada
2) Department of Chemical and Biological Engineering, UBC,
2360 East Mall, Vancouver, British Columbia, V6T 1Z3, Canada

ABSTRACT

An experimental approach is proposed to investigate the gas-solid structure in the vicinity of a sparger nozzle in a fluidized bed. The local hydrodynamics were studied under injection velocities ranging between 0 and 100 m/s and three orientations. A fiber-optic probe was used to measure the instantaneous local particle holdup near the tip of the sparger nozzle. Under the investigated conditions, the local gas-solid structure was influenced by the nozzle orientation and injection velocity and varied according the measurement position. Four distinct zones were identified from the local particle holdup data, with the boundaries corresponding to characteristic jet lengths. Strong discrepancies were found with existing correlations. Further studies are required to achieve better jet length estimation and dynamic analysis of the gas-solid structure.

INTRODUCTION

Gas injection by means of spargers in a fluidized bed reactor is common practice in industrial processes, especially where fast exothermic reactions such as partial oxidation and combustion reactions are taking place (1, 2). For those reactions, spargers play a key role in introducing reactant gases at different locations in the fluidized bed media in order to improve selectivity. Furthermore, the jetting structure often associated with high injection velocities has been reported to considerably intensify the momentum, heat and mass transport (3-6).

Up to now, the understanding and capability of modeling the nozzle region of fluidized beds are limited. The majority of studies carried out on nozzles in fluidized beds focused on upward oriented grid nozzles. As for sparger nozzles, upward oriented sparger nozzles have been studied mostly in jetting fluidized beds (7), while horizontal (8), inclined (9) and downward (1, 2) oriented sparger nozzles were usually studied in fluidized beds. Most studies focused on establishing the boundary

The 12th International Conference on Fluidization - New Horizons in Fluidization Engineering, Vol. 102 [2007]

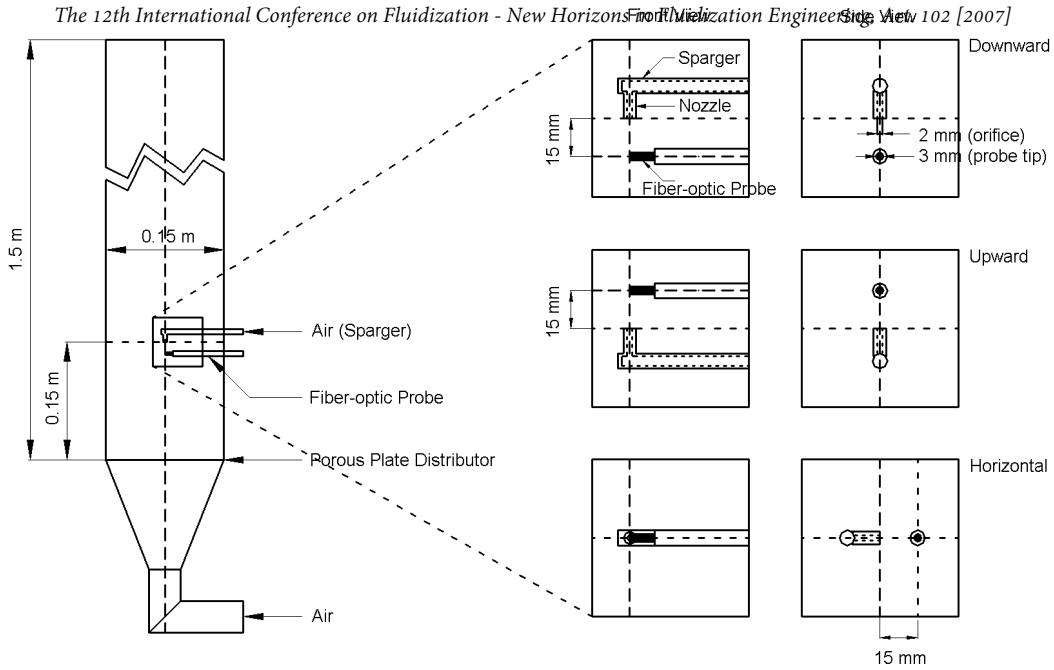

Figure 1 – Schematic diagram of the experimental setup and sparger nozzle/fiber-optic probe configurations

of the jetting structure, mainly the jet penetration length and to a lesser extent its shape (jet half angles). As such, Knowlton and Hirsan's (10) work was instrumental in defining the characteristic jet lengths, namely the minimum jet length (Lj,min), the maximum jet length (Lj,max) and introducing the length corresponding to the deepest penetration of high momentum bubbles originating from the nozzle (Lj,b) where Lj,min<Lj,max<Lj,b. Despite the wide range of experimental approaches that have been used in the past, the majority of the studies yielding correlations have been carried out by visual observation near the wall of two-dimensional and semi-cylindrical fluidized beds.

The purpose of the present study is to investigate the boundary and the gas-solid structure in the vicinity of a sparger nozzle in a fluidized bed of using a fiber-optic probe in a three-dimensional fluidized bed.

EXPERIMENTAL PROCEDURE

Experiments were carried out under ambient conditions in a column with an inner diameter of 0.15 m and a height of 1.50 m. The experimental apparatus is depicted in Figure 1. Air was introduced into the column through a porous plate distributor. FCC particles (Geldart A, ρ_p = 1673 kg/m^3, d_p = 70μm, Φ_{mf} = 0.55, U_{mf} = 0.003 m/s (calculated), U_c = 0.77 m/s (determined experimentally)) were used as bed material. The static bed height was 0.17 m and the superficial gas velocity (U_g) was 0.9 m/s for all experiments. Under operation the bed height reached 0.6-0.8 m. A cyclone mounted on top of the column allowed for the entrained particles to be returned to the fluidized bed. Despite the relatively high superficial gas velocity, the cyclone was sufficiently efficient to allow for the runs to go on without noticeable bed elutriation. A single-nozzle sparger with a 2 mm opening was used for all runs. The nozzle was

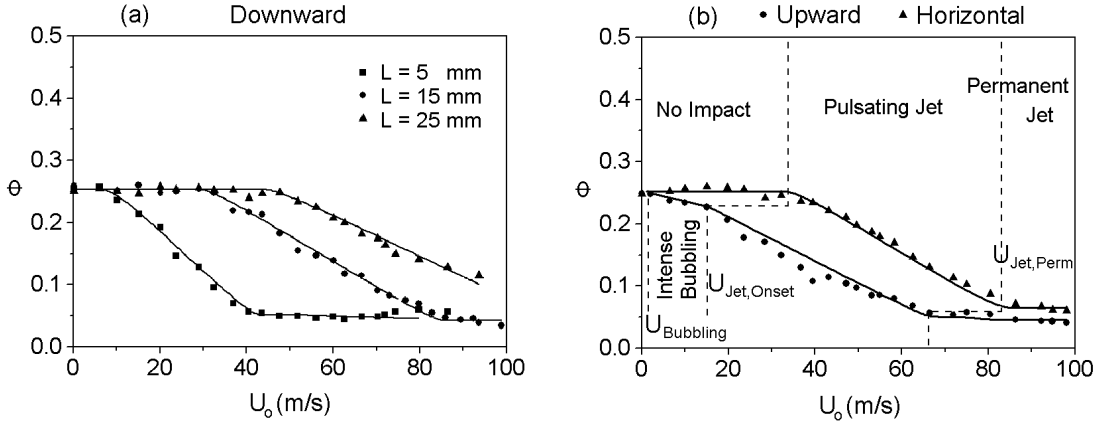

Figure 2 – Influence of injection velocity and measurement distance on the mean particle holdup for three nozzle orientations

positioned at the column center, 0.15 m above the porous plate distributor. The distance between the probe tip and the nozzle opening could be varied and unless specified otherwise, the distance was 15 mm. Inserts in Figure 1 detail the fiber-optic probe/sparger nozzle configurations for all three orientations studied. For each configuration, the injection velocity (U_o) was varied between 0 and 100 m/s. Prior to testing, the fiber-optic probe was calibrated according to the previously published work of Cui *et al* (11).

RESULTS AND DISCUSSION

The results from the runs clearly show that the flow near a nozzle may differ from the bulk of the fluidized bed and often yields a distinct gas-solid structure. This structure can be analyzed in terms of time-averaged and dynamic properties. In the present work, only the results pertaining to time-averaged properties are presented.

Mean Particle Holdup

The mean particle holdup was studied with respect to the measurement location and the injection velocity. These are presented in Figure 2, where (a) shows the results for a downward oriented sparger nozzle for three measurement distances and (b) shows the results from both upward and horizontal oriented sparger nozzles. From figure 2(a), it can be observed that the changes in the average local particle holdup can be generally described by linear relationships between the average local particle holdup and the injection velocity. As the distance between the nozzle and the probe is increased, the trends for all three distances are the same the only change is that the transitions between each linear parts of the curve are pushed towards higher injection velocities. This linear relationship between the solid holdup and injection velocity is also observed in Figure 2(b), where the results from horizontal and upward oriented nozzles are presented.

At low injection velocity (0-10 m/s), the downward and horizontal oriented nozzles show that local particle holdup remains constant, at the same value as when no gas is fed through the nozzle, as if the injected gas had no impact on the fluidized media in the vicinity of the fiber-optic probe. However, the upward oriented nozzle shows a

The 12th International Conference on Fluidization - New Horizons in Fluidization Engineering, Art. 102 [2007]

slightly different behavior as the local particle holdup slowly drops with increasing velocity. This phenomenon is attributed to bubbles originating from the nozzle. The bubble frequency and bubble size increase as the injection velocity is increased, resulting in a lower particle holdup. From the experimental data, it appears that this behavior starts when the injected gas velocity reaches the transition velocity, $U_{Bubbling}$ in the range 0.5-2 m/s. At the measurement location, there is no evidence of intense bubbling with the downward and horizontal oriented sparger nozzles.

As the injection velocity is increased (20-50 m/s), a transition velocity marking the beginning of a more sustained gas penetration is reached. This transition velocity is identified as the jetting onset velocity, $U_{Jet,Onset}$, and when the distance between the nozzle and fiber-optic probe is 15 mm is equivalent to 29, 34 and 15 m/s for the downward, horizontal and upward oriented nozzles, respectively. As the injection velocity is increased, the increased momentum results in more injected gas breaking free through the emulsion phase of the fluidized bed. A jetting structure is periodically forming and this phenomenon continues until a fully sustained injected gas penetration and local domination of the injected gas over the fluidized bed is reached. This transition velocity is identified as the permanent jetting velocity, $U_{Jet,Prem}$, and is equivalent to 84, 85 and 67 m/s for the downward, horizontal and upward oriented nozzles, respectively. The permanent jetting velocity delimits the beginning of a remarkably constant particle holdup for all three orientations (downward oriented nozzle: 0.041; horizontal oriented nozzle: 0.061; upward oriented nozzle: 0.042). The amount of entrained particles inside the jet structure was reported as being the major factor influencing the momentum and heat transfers in the jetting region (3) of fluidized beds. The results suggest that the horizontal oriented nozzle is more prone to particle entrainment as the local particle holdup is greater than for the other two orientations investigated. Further experimental work is required to address this and determine how the bed operating conditions, particle and injected gas properties influence the particle entrainment within the jet structure.

In an effort to consolidate the jet length typically reported from visual observation and the transitions velocities found in this work, four impact zones are defined according to the influence the injected gas has on the fluidized bed. These impact zones have the characteristic jet lengths as their boundaries and are presented in Figure 2(b). The four impact zones are respectively: 1) no impact zone ($L>L_{j,b}$); 2) intense bubbling zone ($L_{j,b}>L>L_{j,max}$); 3) pulsating jet zone ($L_{j,max}>L>L_{j,min}$); 4) permanent jet zone ($L_{j,min}>L$). By varying the injection velocity, while keeping the same sampling position, it is possible to determine the transition velocities for which the distance between the sampling point and nozzle orifice (L) corresponds to a characteristic jet length in the vicinity of a sparger nozzle in a three-dimensional fluidized bed. In other words, when U_o is equal to $U_{Jet,Onset}$, the characteristic jet length $L_{j,max}$ will be equal to L (likewise when $U_o = U_{Jet,Perm} \Rightarrow L_{j,min} = L$ and when $U_o = U_{Bubbling} \Rightarrow L_{j,b} = L$).

Phase specific particle holdup

Since the fluidized bed structure may be described in terms of a dilute and a dense phase, the results are also analyzed with respect to each phase. The segregation of the data into dense and dilute phase elements is achieved based on the minimum probability voidage method (11). The average particle holdup in the dilute phase, changes with increasing injection velocity, following similar trends as observed with

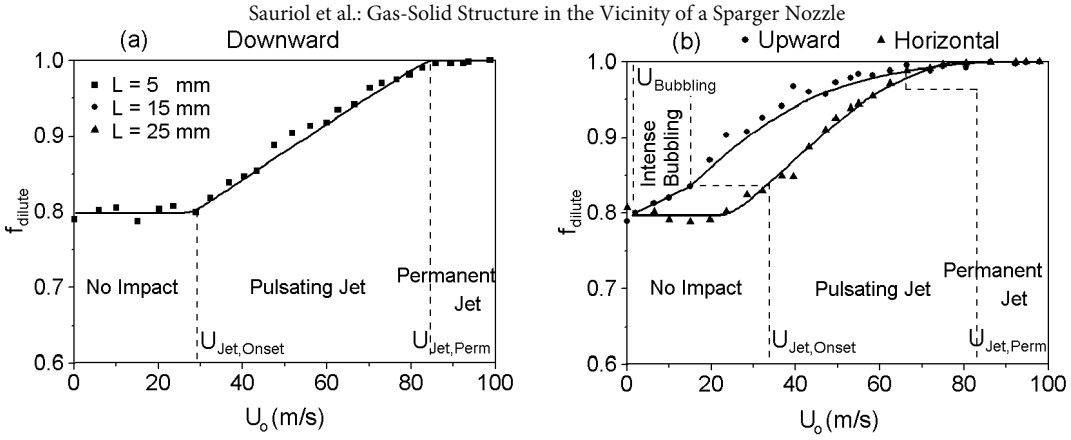

Figure 3 – Influence of injection velocity on the dilute phase fraction for three nozzle orientations

the mean particle holdup presented in Figure 2. On the other hand, the dense phase particle holdup remains almost constant throughout the range of injection velocities investigated for all three nozzle orientations, ranging from 0.50 at low injection velocity to 0.45 at high injection velocity. In order to complement this analysis, the dilute phase fraction was computed and the results are presented in Figure 3. The dilute phase fraction reflects the probability of the dilute phase to exist at the measurement location. The observed trends are similar to those of Figure 2, with transition velocities near the locations where the dilute fraction changes slope. However near the $U_{Jet,Perm}$ transition for all three orientations but most noticeable with the upward oriented nozzle, the dilute phase fraction breaks from linearity and approaches unity asymptotically.

Correlations from the Literature

The experimental transition velocities and corresponding jet lengths are compared to existing correlations from the literature. The correlations and results are presented in Table 1.

In most cases, important discrepancies exist between the calculated jet lengths and the measurements. These discrepancies can often be attributed to the simplicity of the correlations which do not always incorporate the system properties and operating conditions. For example, only two out of ten account for the superficial gas velocity and only six for the particle size diameter. Another source of discrepancy comes as a result of the limited number of correlations. In fact most correlations are based on experimental data from Geldart B and D particles, using them for Geldart A particles results in coarse extrapolations of certain terms. Overall the best agreement is achieved when calculating $L_{J,max}$ for a downward oriented sparger nozzle using the correlation proposed by Yates *et al* (1), which was derived from tests with similar particles and operating conditions.

CONCLUSION

In an effort to investigate the gas-solid structure in the vicinity of a sparger nozzle, a fiber optic probe was used to measure the instantaneous local particle holdup near

Table 1 – Comparison between experimental jet length and correlations

Orientation	Author	Correlation	U_o (m/s)	L (mm)	
				Exp.	Cal.
Downward	Zenz (12)	$\frac{L_{j,max}}{d_o}=22.73\times\log_{10}\left(U_o\sqrt{\rho_g}\right)-35.61$	7	5	<0
			29	15	<0
			46	25	6.1
	Yates *et al* (1)	$\frac{L_{j,max}}{d_o}=2.8\left(\frac{\rho_g}{\rho_p-\rho_g}\frac{U_o^2}{gd_o}\right)^{0.4}$	7	5	7.2
			29	15	22
			46	25	32
Upward	Zenz (12)	$\frac{L_{j,max}}{d_o}=69.44\times\log_{10}\left(U_o\sqrt{\rho_g}\right)-96.30$	15	15	<0
	Luo *et al* (9)	$\frac{L_{j,max}}{d_o}=119\left(\frac{U_o^2}{gd_o}\right)^{0.18}\left(\frac{\rho_p U_o d_p^2}{\mu_g d_o}\right)^{-0.024}\left(\frac{\rho_g}{\rho_p}\right)^{0.49}$	15	15	31
	Hirsan *et al* (13)	$\frac{L_{j,b}}{d_o}=26.6\left(\frac{\rho_g}{\rho_p}\frac{U_o}{\sqrt{gd_p}}\right)^{0.67}\left(\frac{U_g}{U_{cf}}\right)^{-0.24}$	0.5-2	15	0.8-1.9
	Hirsan *et al* (13)	$\frac{L_{j,max}}{d_o}=19.3\left(\frac{\rho_g}{\rho_p}\frac{U_o}{\sqrt{gd_p}}\right)^{0.83}\left(\frac{U_g}{U_{cf}}\right)^{-0.54}$	15	15	0.8
	Masmurra (14)	$\frac{L_{j,b}}{d_o}=3.0\left(\frac{U_o^2}{gd_o}\right)^{0.32}\left(\frac{\rho_g U_o d_p}{\mu_g}\right)^{-0.37}\left(\frac{\rho_g}{\rho_p}\right)^{-0.33}\left(\frac{d_p}{d_o}\right)^{0.24}$	0.5-2	15	48-70
Horizontal	Zenz (12)	$\frac{L_{j,max}}{d_o}=69.44\times\log_{10}\left(U_o\sqrt{\rho_g}\right)-96.30$	34	15	0.8
	Merry (7)	$\frac{L_{j,max}}{d_o}=5.25\left(\frac{\rho_o}{(1-\varepsilon)\rho_p}\frac{U_o}{\sqrt{gd_o}}\right)^{0.4}\left(\frac{\rho_g}{\rho_p}\right)^{0.2}\left(\frac{d_p}{d_o}\right)^{0.2}-4.5$	34	15	1.2
Inclined and horizontal	Hong *et al* (8)	$\frac{L_{j,max}}{d_o}=1.64\times10^6\left(\frac{\rho_o}{(1-\varepsilon)\rho_p}\frac{U_o}{\sqrt{gd_p}}\right)^{0.327}\left(\frac{\rho_g}{\rho_p}\right)^{1.974}\left(\frac{d_p}{d_o}\right)^{-0.040}\times\left(\frac{\alpha\pi}{180}+\frac{\pi}{2}\right)^{0.148}\left(\frac{h_o}{h}\right)^{0.028}-3.80$	34	15	34

the tip of a single sparger nozzle. The results of the experimental work exhibited noticeable characteristics that helped analyze the local gas-solid structure. The local flow structure in the vicinity of a sparger nozzle in a fluidized bed depends strongly on the injection velocity and orientation. Four impact zones were defined: at low injection velocities, the no impact zone; with slightly higher injection velocity, the intense bubbling zone (for the upward oriented nozzle only); at intermediate injection velocities, the pulsating jet zone; at high injection velocities, the permanent jet zone. The boundary of these zones corresponding to the characteristic jet lengths that are typically reported from visual observation. On a time-averaged scale, the gas-solid structure showed linear relationship between the hydrodynamic properties (mean particle holdup, particle holdups in the dilute phase and dilute phase fraction (for downward)) and the injection velocity. Transition velocities, $U_{Bubbling}$, $U_{Jet,Onset}$ and $U_{Jet,Perm}$, were easily determined from the mean particle holdup data.

The experimental jet lengths were compared with existing correlations. The particle size appears to have a great influence on the predicted jet lengths. In general, correlations developed for fluidized beds of coarse particles (Geldart B and D) are not well suited for fine particles (Geldart A). Another drawback from the correlations is that the influence of the fluidizing velocity is not always taken into account since most of them were developed for incipiently fluidized beds. Further investigations

are required in order to offer better jet length estimation and dynamic analysis of the gas-solid structure.

ACKNOWLEDGEMENTS

The authors gratefully acknowledge the Postdoctoral Fellowship (2000-2002) awarded to Heping Cui by the Natural Sciences and Engineering Research Council of Canada (NSERC), and also the work and technical assistance of Mr. Jean Huard.

NOTATION

Variables
d = diameter (m)
f = phase fraction (-)
g = gravitational constant (m/s^2)
h = height (m)
L = length (m)
U = velocity (m/s)

Greek letters
α = nozzle inclination angle (º)
ε = bed voidage (-)
μ = viscosity (Pa·s)
ρ = density (kg/m^3)
Φ = particle holdup (-)

Subscripts
Bubbling = intense bubbling transition
c = transition to turbulent
cf = complete fluidization
dilute = dilute phase
g = superficial gas
Jet,Onset = jet onset transition
Jet,Perm = permanent jet transitions
j,b = high momentum jet bubbles
j,max = maximum jet
j,min = minimum jet
mf = minimum fluidization
o = orifice
p = particle

REFERENCES

1. Yates, J.G., Cobbinah, S.S., Cheesman, D.J. and Jordan, S.P. (1991). Particle Attrition in Fluidized Beds Containing Opposing Jets. AIChE Symposium Series, 87, 13-19.
2. Sotudeh-Gharebaagh, R. and Chaouki, J. (2000). Gas Mixing in a Turbulent Fluidized Bed Reactor. Canadian Journal of Chemical Engineering, 78(1), 65-74.
3. Donadono, S. and Massimilla, L. (1978). Mechanisms of Momentum and Heat Transfer between Gas Jets and Fluidized Beds. In J. F. Davidson and D.L. Keairns, Fluidization, (p. 375). New York: Engineering Foundation.
4. Gbordzoe, E.A.M. and Bergougnou, M.A. (1990). Mass Transfer from a Central Jet Introduced into a Large Two-Dimensional Fluidized Bed. Powder Technology, 62(1), 67-75.
5. Molodtsof, Y. and Labidi, F. (1995). Jets in Fluidized Beds: Flow Structure and Gas Mixing. In G. Laguéri and J. Large, Fluidization, vol. VIII (p. 279). New York: Engineering Foundation.
6. Bi, J. and Kojima, T. (1996). Prediction of Temperature and Composition in a Jetting Fluidized Bed Coal Gasifier. Chemical Engineering Science, 51(11), 2745-2750.
7. Merry, J.M.D. (1971). Penetration of a Horizontal Gas Jet into a Fluidized Bed. Transactions of the Institute of Chemical Engineers, 49, 189-195.
8. Hong, R., Li, H., Li, H. and Wang, Y. (1997). Studies on the Inclined Jet Penetration Length in a Gas-Solid Fluidized Bed. Powder Technology, 92(3), 205-212.

9. Luo, G., Zhang, J.-Y., Guo, Q. and Zhang, B. (1999). Study on Jet Flow from Two Vertical Nozzles in a 500 mm I.D. Semi-circular Fluidized Bed. Chemical Engineering and Technology, 22(3), 247-251.
10. Knowlton, T.M. and Hirsan, I. (1980). The Effect of Pressure on Jet Penetration in Semi-cylindrical Gas-fluidized Beds. In J.R. Grace and J.M. Matsen, Fluidization, (p. 315). New York: Plenum Press.
11. Cui, H., Mostoufi, N. and Chaouki, J. (2001). Gas and Solids between Dynamic Bubble and Emulsion in Gas-fluidized Beds. Powder Technology, 120(1-2), 12-20.
12. Zenz, F.A. (1968). Bubble Formation and Grid Design. I. Chem. E. Symposium Series, 30, 136-139.
13. Hirsan, I., Sishtla, C. and Knowlton, T.M. (1980). The Effect of Bed and Jet Parameters on Vertical Jet Penetration Length in Gas Fluidized Beds. 73rd Annual AIChE Meeting.
14. Masmurra, D. (2000). Influence of Particle Size and Density on the Jet Penetration Length in Gas Fluidized Beds. Industrial Engineering Chemistry and Research, 39(7), 2612-2617.